FUDMA Journal of Sciences (FJS)
ISSN online: 2616-1370
ISSN print: 2645 - 2944
Vol. 9 No. 12, December (Special Issue), 2025, pp 273 – 280
DOI: https://doi.org/10.33003/fjs-2025-0912-4016

DESIGN AND SIMULATION OF A NOISE TO ELECTRICAL ENERGY CONVERTER USING PIEZOELECTRIC TRANSDUCERS

***Iliya Favanza Kwaha, Augustine Anuhu Habila and Danladi Ali**

Department of Pure and Applied Physics, Adamawa State University, Mubi, Adamawa State, Nigeria.

*Corresponding authors' email: iliya1215@adsu.edu.ng

ABSTRACT

With global technological advancement and increasing energy demand, especially in developing economies like Nigeria, there is a growing need for sustainable and decentralized micro-power generation systems. Noise energy harvesting offers a renewable approach to supplement conventional electricity supply. This study aims to design and simulate a compact system for converting ambient noise into usable electrical energy using a piezoelectric transduction mechanism. A simulation model was developed in Proteus 8 environment, comprising piezoelectric transducer mesh, Half-Wave Cockcroft–Walton voltage multiplier, control/charging unit, 12V battery and an inverter unit. The mesh generated a peak voltage of 9.5V, which was multiplied to 19V and regulated to a stable 12V for charging a 12V battery. The inverter produced an output power of 1kVA with an estimated efficiency of 82.6%, sufficient to power small home appliances such as laptops, phone chargers and lighting systems. The system exhibited good voltage stability under varying noise intensities, demonstrating its potential as a supplementary renewable energy source. Overall, this study contributes to the development of noise-based micro-power systems suitable for low-energy applications, offering a pathway toward improved energy sustainability and urban renewable integration.

Keywords: Piezoelectric, Transducers, Noise, Voltage multiplier and Controller

INTRODUCTION

Electrical energy is the prime mover of any economy. It is the engine of growth around which all sectors of the economy revolve (Nkwocha et al., 2024). Despite the variety of conventional and renewable energy options (solar, nuclear, biomass, wind, geothermal, hydroelectric, wet geothermal, tidal, ocean energies and diesel/gasoline generators), global supply remains insufficient, particularly in sub-Saharan Africa (Onuu, 2020). In Nigeria, population growth and industrialization have intensified the energy demand-supply imbalance (Kenneth and Ibe, 2010). As at 2015, the share of renewable energy source in electricity generation in Nigeria was around 23.7%; with 16.6% coming from hydropower, 3.7% from wind and 3.4% from other new renewables (Akorede et al., 2017; Oluwatoyin, 2023). Because of the limited sources of electricity in these countries and large population/ increase in economic activities, electricity outage in the residential, commercial and industrial sectors are on the constant rise: causing off-grid power generation by individuals and corporate bodies. This off-grid power generation increases the carbon footprint, prices of goods and services of these countries.

Given the widening energy deficit and environmental degradation from fossil fuels, harvesting ambient acoustic energy(noise) offers a sustainable complement to existing renewables. Noise is an unpleasant sound that possess energy. It is harmful to human beings and thus, it is regarded as pollutant. As a risk factor that has harmful effects on the human body, it leads to disturbances of the organ of hearing, negative social behavior, annoyance, sleep disorder, reduction in labour productivity and intelligibility of speech (Najimaldin, 2024). Noise is not restricted to specific areas though it is much in places like: airports, railways tracks, parties, industries, construction sites and markets (Pantawane et al., 2017).

In an attempt to reduce power outage (electrical energy) and wastage of acoustic energy, research on conversion of noise to electrical energy by scientist worldwide is ongoing: they seek to bring out technologies that are beneficiary to humans through proper utilization of the energy from the surroundings (Poornanand et al., 2017; Suhas et al., 2019). One of such technology is the use of piezoelectric transducers.

Piezoelectric transducer is a crystal that can convert mechanical strain to electricity. When a piezoelectric crystal is placed in an electric field, or when charges are applied by external means to its faces, the crystal experience changes in its dimensions (strain). When the direction of the strain reverses, the polarity of the electric charge is reversed (piezoelectric effect) and when the direction of the electric filed is reversed, it causes a reverse in the direction of the resulting strain (inverse piezoelectric effect) (Shalabh, 2012). This piezoelectric effect, arises from non-centrosymmetric crystal structures, where applied stress displaces charge centers, generating an electric potential proportional to the mechanical strain. The ability of this Piezoelectric transducers to develop electric charges in response to an applied mechanical stress is known as Piezoelectric electricity. These Crystals can be obtained naturally (Quarts, Cane Sugar, Topaz and Tourmaline) or artificially (Zinc Oxide, Lead Niobate, Potassium Niobate and Sodium Niobate) (Satvik et al., 2020). When sound energy (Noise) is applied to a piezoelectric crystal, it creates and reverse the strain. The strain is then converted into electrical energy. This piezo electriceffect of a piezoelectric crystal is what is used in the conversion of sound energy to electrical energy (Poornanand et al., 2017).

Urban sound pressure levels often exceed 85dB, corresponding to acoustic energy densities sufficient to induce unregulated microvolt-level potentials in piezoelectric devices. Thus voltage boosters and control mechanisms have to be deployed to effectively utilized the piezoelectric transducer technology.

Revathi and Ingitham (2012) researched on "piezoelectric energy harvesting system in mobiles with keypad and sound vibrations". The paper targeted the transformation of mechanical and sound energy to electrical energy using piezoelectric materials. Based on their simulation results, a voltage of 4.26V was generated. This voltage however is too small and one needs to be constantly pressing the keypads.

While Dhananjay et al. (2014) in their paper "piezoelectric energy harvester design and power conditioning" improved voltage output using floor tiles to 5.0v, their approach required continuous physical interaction. Thus, limiting scalability. The work of Niraj et al. (2014) on "footstep energy harvester using piezoelectric transducer" improved the output voltage by using a piezo panel with 16 piezoelectric transducers. However, the problem of continuous physical interaction and scalability were not addressed. Their system required people to matched the panel for a long period of time (4-5 days): making it impossible for the system to work in residential areas. Kyrillos et al. (2016) in their paper "acoustic energy conversion into useful electric energy from disk jockey by using piezoelectric transducers" achieved higher voltage (28V) under acoustic excitation but without voltage stabilization mechanisms. This problem was resolved by Anis et al. (2019) in their work "power generation by using piezoelectric transducer with bending mechanism support". They employed 3D printer technology to support the piezoelectric transducer during deflection process. This has significantly increased the voltage to 34.4v. This voltage however is not sufficient to power electronic gadgets like Tv Set. Thus the need to improve on the output voltage.

This study introduces an integrated control mechanism for stabilizing piezoelectric-generated voltage, addressing efficiency and reliability. It also integrated an inverter to increase the output voltage. Thus solving the challenges of prior designs.

MATERIALS AND METHODS

Methods of circuit design and simulation techniques were used in this study. The block diagram of Fig.1 shows how the various parts interact and interface with each other to give the required output. The design and selection of the various components and stages were guided by performance targets (efficiency and voltage stability) and availability of components in the local market.

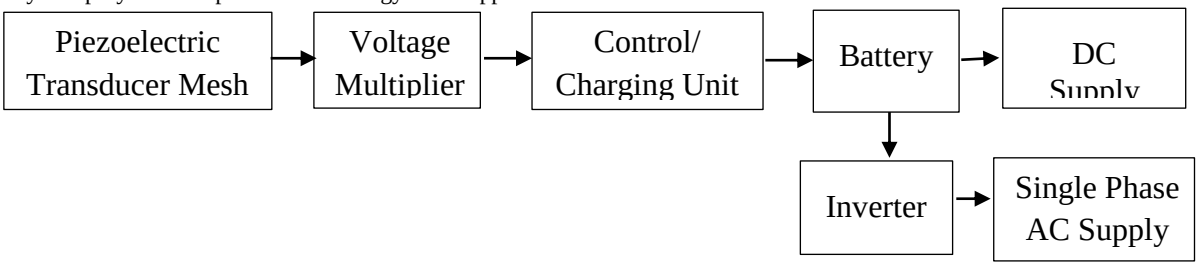

Figure 1: Block Diagram of the Noise to Electrical Energy Converter

The design procedure followed the block diagram of Fig.2. It started with the Piezoelectric Transducer Mesh and ended with the Inverter stage. The following subsections, gave a detailed chronological design order of each stage and the simulation of the entire system.

Design of the Piezoelectric Transducer Mesh

A piezoelectric transducer is represented electrically by a current source (I) connected in parallel to the capacitance of the piezoelectric plate (C) as demonstrated by Wang et al. (2017) in equation 1

$$i(t) = -A\frac{dp}{dt} + C\frac{dV}{dt} \quad (1)$$

Where A is the area of the piezoelectric transducer, t is the thickness, p(t) is the incident sound pressure, C is the capacitance and i(t) is the current. In this project, 7BB-20-6C piezoelectric transducer was used. From its data sheet, C= 8.5uF, R= 500Ω and f = 6.3kHz. 6 of such piezoelectric transducer were connected in parallel in a group of four that are then connected in series to give a total of 24 piezoelectric transducers with an output voltage of 9.5v as shown in Fig. 2.

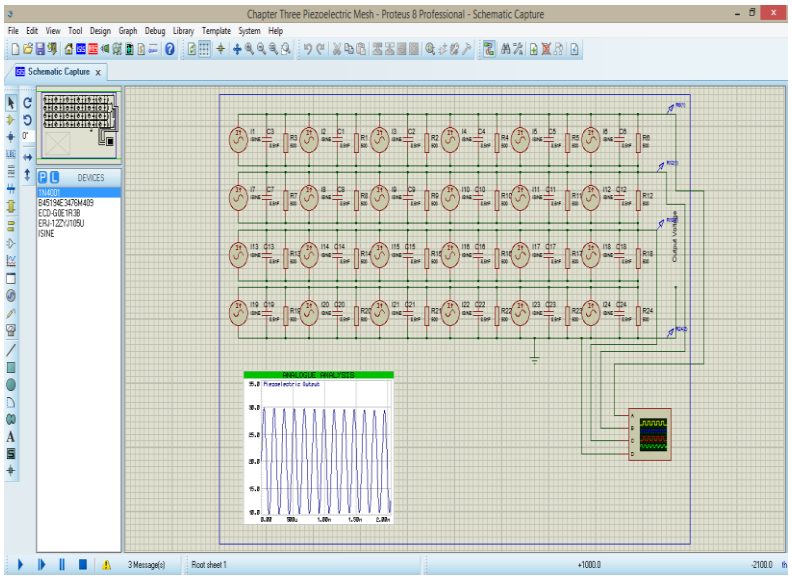

Figure 2: Piezoelectric Transducer Mesh Showing Hybrid Connection

Design of the Voltage Multiplier Unit

The voltage generated by the piezoelectric transducer mesh is small and is not constant. A voltage multiplier that will allow the Control/Charging unit to have sufficient voltage was included. The voltage multiplier that was used in this project was the 'Half-Wave Cockcroft- Walton Voltage multiplier shown in Fig.3.

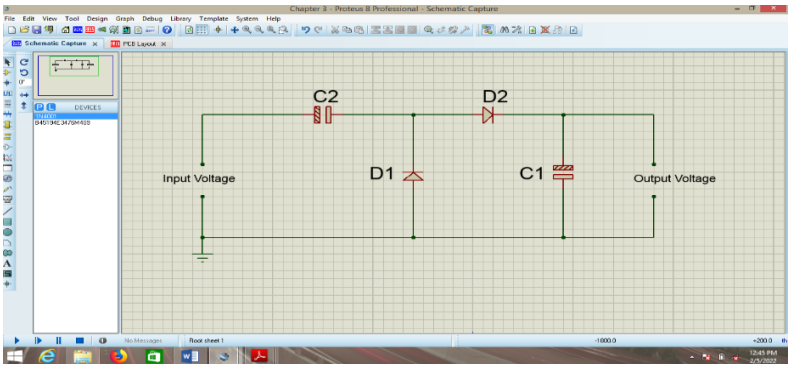

Figure 3: Schematic of The Half-Wave Cockroft- Walton Voltage Multiplier

Capacitor C_2 selection

The Capacitor C_2 is given as:

$$C_2 \geq 2\left(\frac{V_{in}-V_\gamma}{R.\Delta V_{out}f}\right) \quad (2)$$

Where V_{in} is the amplitude of the input Voltage, V_γ is the diode Knee Voltage, ΔV_{out} is the output ripple voltage, f is the frequency of the input voltage and R is the Load. Using V_{in} = 9.5v (Voltage from the piezoelectric mesh), V_γ = 0.8V, ΔV_{out} = 2v, f = 300kHz and R =100Ω in equation 2, C_2 was selected as 22µF

Capacitor C_1 selection

The Capacitor C_1 is given as:

$$C_1 = -\frac{i_{C_1 disc}(f^{-1}-t_{disc})}{\Delta V_{C_1}} \quad (3)$$

Where $i_{C_1 disc}$ is the current of capacitor C_1 during discharging, t_{disc} is the discharging period . With the values of f = 300kHz, $\Delta V_{C_1} = -0.9883V$, $t_{disc} = 3.2879237 * 10^{-6}\ s$ and $i_{C_1 disc} = 975.8338$ A in equation 3, C_1 was selected as 47 µF.

Diode D1 and D2 selection

In selecting the diodes, the suggestions of (Kenneth and Ibe, 2010) was adhered to. 1N4001 was chosen.

Design of the Control / Charging Unit

Because the Voltage Multiplier only multipliers whatever voltage is applied at its input above 8.5v, there's need for the output of the multiplier to be controlled so as to give a constant output voltage. The schematic of the regulation and charging unit is given in Fig.4.

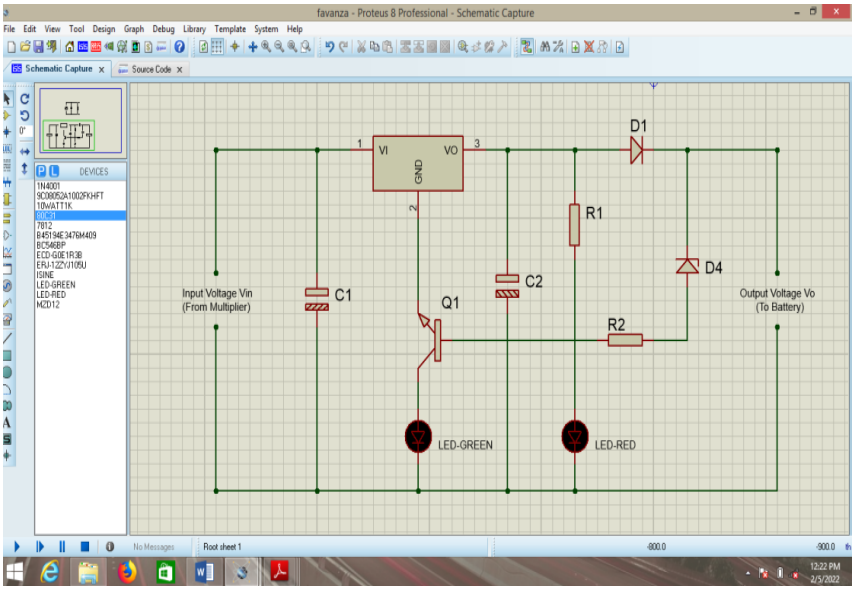

Figure 4: Schematic Of The Regulation/ Charging Unit

Capacitor C_1 selection

A Ceramic capacitor C_1 was selected to reduce the ripple voltage amplitude seen at the input. C_1 in µF was calculated from:

$$C_1 = \frac{I_{out} * dc*(1-dc)*1000}{f_s * V_p} \quad (4)$$

Where f_s is the switching frequency in kHz, I_{out} is the steady state output load current, V_P is the maximum allowed peak-peak ripple voltage, η is the efficiency and dc is the duty cycle. In this design, V_{out} = 12v, I_{out} = 7A, V_{in} = 16.8 v , V_p = 75mV, f_s = 300kHz, $dc = 0.79365$ and with η = 90%. C_1 was selected as 47µF.

LM 780 IC

Directly connecting the voltage multiplier to the battery may explode it due to the varying output as a result of varying inputs. To avoid such, a controller (voltage regulator IC) is used. The voltage that comes from the voltage multiplier is actually greater than or equal to 17v DC. This voltage is now controlled by a fixed positive LM 780 IC to 12v which is sufficient to charge the 12v battery for this project.

Capacitor C_2 Selection

Capacitor C_2 provides further smoothening after the voltage has been regulated. Its value was calculated as:

$$C_2 = \frac{I_{out}}{4\sqrt{3} * f * V_p} \quad (5)$$

With , I_{out} = 7A, V_p = 74mV and f_s = 300kHz in the equation (5), C2 = 47uF was selected.

Current Limiting Resistor R_1 Selection

The current limiting resistor R_1 provides protection to the Red LED (the Red LED is an indicator used in this project to indicate that the battery is charging). The value R_1 was calculated from:

$$R_1 = \frac{V_{out} - V_{Red}}{I_{Red}} \quad (6)$$

Where V_{Red} and I_{Red} are the voltage and current across the Red LED respectively. With V_{Red}= 2v I_{Red} = 20mA and V_{out} = 12v, in equation (6), $R_1 = 500\Omega$ was selected

Diode D_1 Selection

The diode D1 stops the discharge of the battery back to the regulation unit. In this design, 1N40001 diode was used because it can handle this circuit requirement.

Battery Protection Unit

This part consists of R_2, BC547, Zener Diode ZD and Green Led. It prevents the battery from overcharging. The transistor is serving as a switching device. Once there's reverse voltage across the Zener Diode (in this case 12V), The resistor R_2 set the transistor into operating in the hard saturation region, causing it to draws all the current and thus, protecting the battery from overcharging. R_2= 10kΩ was found to be sufficient. The Green Led was placed to indicate that the battery is fully charged (12V).

Design of the Inverter Unit

At this stage, The DC 12v from the battery is convert into an AC voltage 200v. The stage consists of the oscillation, switching, regulation and amplification stages. The schematic of the inverter designed in this circuit is given in Fig.5.

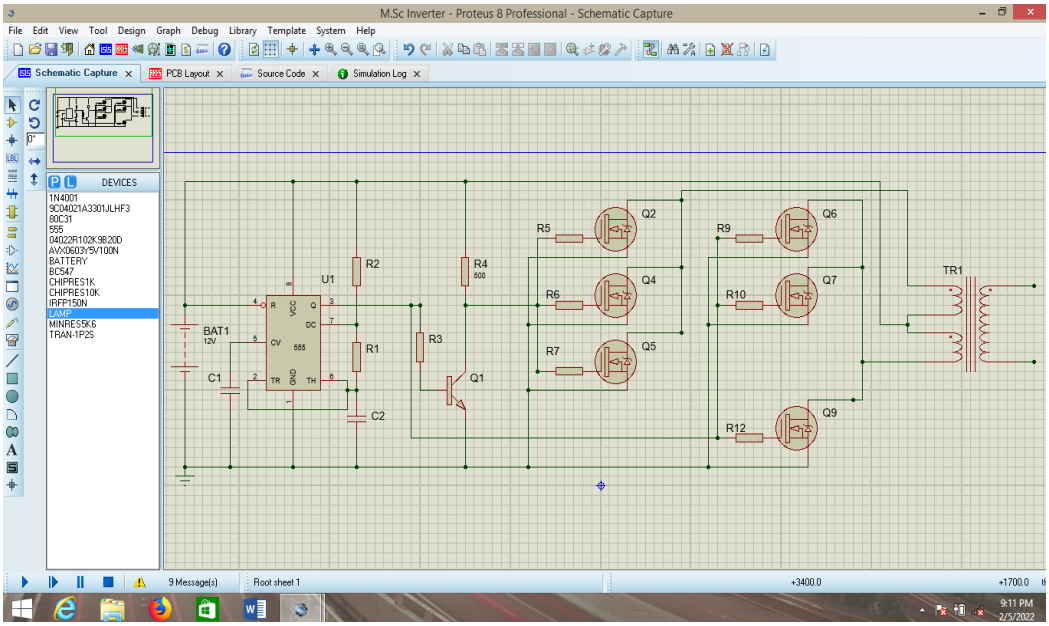

Figure 5: The Schematic Of The Inverter Unit

Oscillation Stage Selection

At this stage that the DC voltage is converted to a digital signal. The 555 timer IC was selected to work as an astable multivibrator at a duty cycle of 50%. With C_2=10nF and frequency f = 50Hz, $R_1 = 1.44M\Omega$ and $R_2 \geq 18.73k\Omega$ were obtained from equation 7.

$$f = \frac{1.45}{(R_2 + 2R_1)C_2} \quad and \quad R_2 \geq 0.013R_1 \quad (7)$$

Transistor Selection (Switching)

Transistor 2N2222 was selected and operated in the extreme region to serve a switching and linear amplification circuit. From transistor 2N2222 data sheet, I_C = 30mA and h_{FEmin} = 100. For $V_{HIGH} = V_{CC}$ = 12V. R_c =18.73kΩ was selected and for saturation, $R_B = 1.44M\Omega$ was selected

MOSFET Switch Selection (Regulation) and Transformer Selection (Amplification)

The MOSFET here is also operated as a switch in it cut-off and saturation region. From MOSFET data sheet, V_{GS} = 7v, I_G = 20mA. For V_{HT} = 12V. $R_G = 250\Omega$ was selected. A 12V-0-12V set-up transformer was selected (Center tapped 24v) to give an output power of 1kVA. Thus from, $V_s I_s = V_p I_p$, $I_p = 84A$. To shoulder this current at the primary as heat, three MOSFET stages were used: each shouldering 28A.

Simulation of the Noise to Electrical Energy Converter

After the first objective (design and cascading of the various blocks) was achieved, the complete system was then designed in the workspace of Proteus 8 as shown in Fig.6 in other to achieve the second objective. An oscilloscope was attached to the design to show the output voltage of the system.

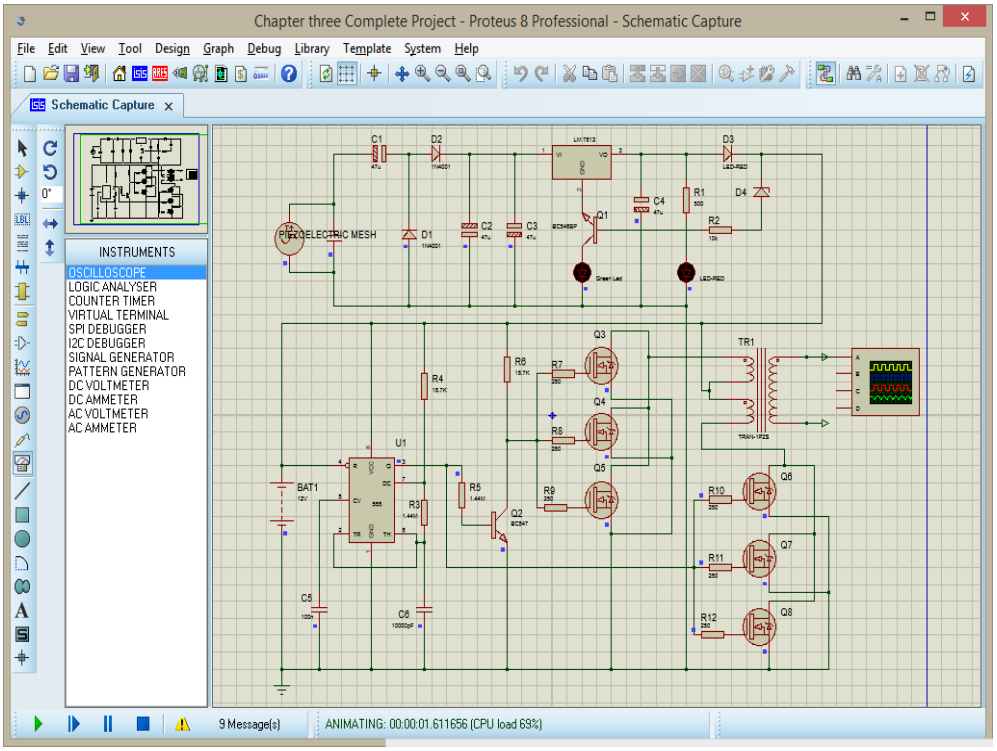

Figure 6: Simulation of Complete Circuit of the Noise to Electrical Energy Converter

The comprehensive materials' list including part numbers, specifications, and manufacturer details of the designed system are shown in Table 1.

Table 1: Component Description, Manufacturer/Band and Manufacturer Part Number

B	Description	Manufacture Part Number	Manufacturer / Brand
1	Capacitor C1, C3, C4 — 47µF	KEMET T495D476M035AT	KEMET / Nichicon / Panasonic
2	Capacitor C2 — 22µF	Panasonic EEUFM1A220	Panasonic / Nichicon
3	Capacitor C5 — 100nF	Murata GRM32 100nF	Murata / TDK / AVX
4	Capacitor C6 — 10,000pF	TDK C3225X5R1H103K	TDK / Murata
5	Diode D1, D2 — 1N4001	ON Semiconductor 1N4001	ON Semiconductor / Vishay
6	Resistor R1 — 500Ω	Yageo RT0603FRD07100R	Yageo / Vishay
7	Resistor R2 — 10kΩ	Vishay CRCW080510K0FKEA	Vishay / Yageo
8	Resistor R3, R5 — 1.44MΩ	KOA Speer RK73H1.44M	KOA / Vishay
9	Resistor R4, R6 — 18.7kΩ	Vishay CRCW080518K7FKEA	Vishay / Yageo
10	Resistors R7–R12 — 250Ω	Vishay CRCW0805250R0FKEA	Vishay / Yageo
11	Transistor Q1, Q2 — BC547	ON Semiconductor BC547B	ON Semiconductor / NXP
12	LED 1 (Red)	Kingbright WP710A10SRD	Kingbright / OSRAM
13	LED 2 (Green)	Kingbright WP710A10SGD	Kingbright / OSRAM
14	Voltage Regulator — LM7812	ST L7812CV	STMicroelectronics / TI
15	MOSFET Q3–Q8 — IRFP150N	Infineon IRFP150N	Infineon / ON Semiconductor
16	Timer IC — 555	Texas Instruments NE555P	Texas Instruments / ON Semi
17	Battery — 12V	Panasonic LCR127R2P	Panasonic / Yuasa
18	Piezoelectric Transducer — 7BB206C	Murata 7BB206C	Murata Electronics
19	Wires	Alpha Wire 2774 22AWG	Alpha Wire / Belden
20	PCB	2layer FR4, 1.6mm	JLCPCB / PCBWay
21	Transformer 12→240V Step-up	Triad Magnetics N14712	Triad / Hammond

In carrying our reliability and validation analysis (align the study with standard engineering evaluation protocols) the methods of Kadandani et al., (2023); Koteras and Tomczuk (2024); Zaharaddden, and Aliyu (2025) and Predescu and Ronu (2025) were adopted. In testing the system under ideal condition (simulation environment), the equivalent power ratings of Laptop, 40Watts bulb and Handset charger were used as loads attached to the system.

RESULTS AND DISCUSSION

After the simulation of the designed system, the following results were obtained and displayed based on the output of the analog analysis graph, Distortion analysis, DC and AC sweep analysis.

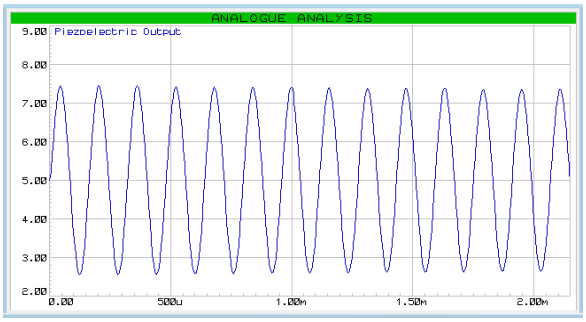

Figure 7: 6 PZT in Parallel

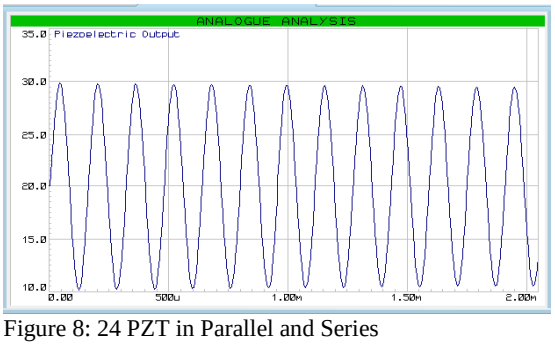

Figure 8: 24 PZT in Parallel and Series

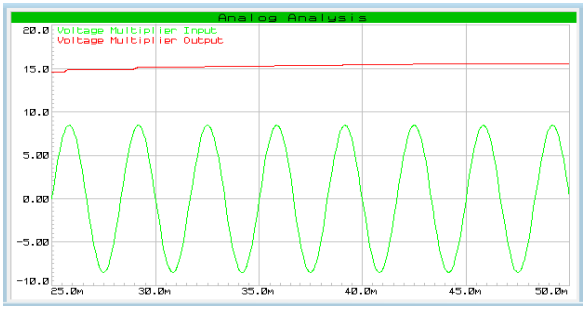

Figure 9: Voltage Multiplier at Input of 8.5v

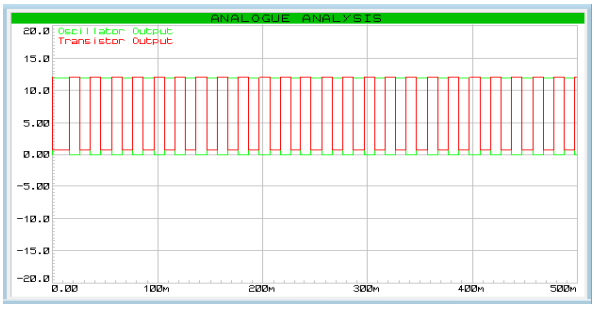

Figure 10: Oscillator and Switching Transistor

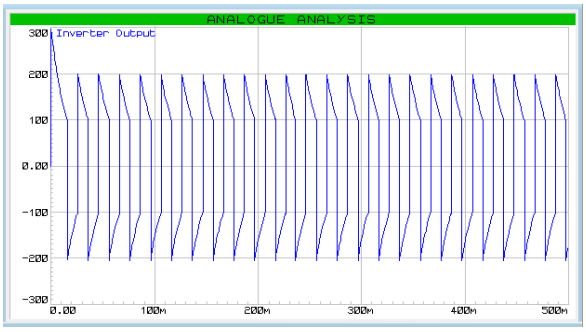

Figure 11: Inverter Voltage 0utput 200v

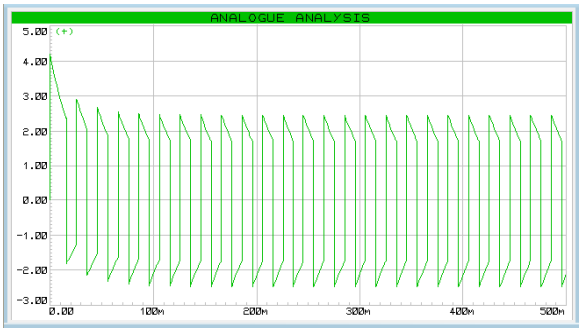

Figure 12: Inverter Current Output 5A

Figure 7 shows the output of 6 piezoelectric transducers connected in parallel to each other. The output shows a good sine wave with a crest voltage of 2.6v and trough voltage of 2.6v. This voltage however, is too small to power the designed system. Even when the voltage is multiplied by the voltage multiplier, it will not be sufficient (5.2v). The number of piezoelectric transducers was increased so as to increase the voltage. As such, 24 piezoelectric transducers grouped into four with each group containing 6 piezoelectric transducers connected in parallel to each other. The four groups are then connected in series to each other. Fig.8 shows this arrangement having a crest voltage of 9.5v and trough voltage of 9.5v. This voltage is sufficient enough to power the designed system.

This 9.5v (24 Piezoelectric transducers) was given to the voltage multiplier as input and an output DC voltage of 18.5v was recorded (97.36% multiplication) as shown in Fig.9. The 97.36% multiplication efficiency indicates minimal diode and capacitor losses, validating the use of a Half-Wave Cockcroft–Walton circuit for low-frequency vibration energy harvesting. The 18.5V output achieved surpasses the 4.26–17 V range reported by Revathi and Ingitham (2012); Dhananjay et al. (2014) and Niraj et al. (2014). Demonstrating the improved performance of multi-array piezoelectric configurations under controlled simulation conditions.

Fig.10 shows the output of the oscillator section of the designed inverter and the output of the switch transistor. It can be seen that the ON state is at 12v and the OFF state at 0v. The switch transistor takes the output of the oscillator and gives it a phase shift of 180^0 such that when the output of the oscillator is ON, the output of the transistor is OFF and when the output of the oscillator is OFF, the output of the transistors shifts to ON state.

Fig.11 shows the maximum output voltage of the designed system which is 200v while Fig.12 shows the maximum current that can be generated by this device which is 5A. The output of the designed system at different battery level (1v-12v) was observed. It was seen that at low voltage value of the battery (1v to 4v), there were lots of distortions and the output loses it AC waveform(shape). The AC nature of the output was restored at battery level of 5v - 6v. However, the output at these voltages though being AC (85v and 90v at 5v and 6v battery levels respectively), is still too weak to power effectively most of the home electric appliances which requires at least 100v. But, at battery voltage of 7v and 8v, the AC out voltage is increased to 100v and 110v respectively. At battery level of 9v-12v, there was a quantum leap in the output AC of 140v, 150v, 180v and 200v respectively. This is depicted in Fig. 13.

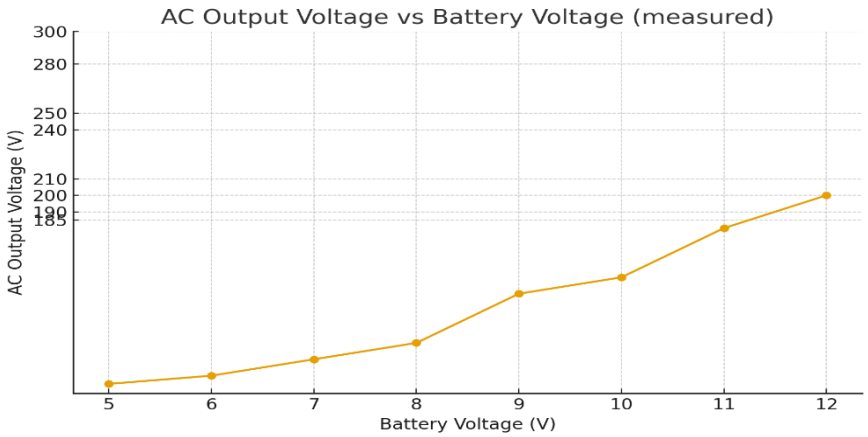

Figure 13: AC Output Voltage Against Batter Voltage

Table 2: Design Reuslts Verses Simulation Results

Description				
Stages/ units	**Designed Values**		**Simulation Values**	
	Input	**Output**	**input**	**Output**
PZT Mesh	85db	8.5V	85db	8.5V
Voltage Multiplier	8.5V	17V	8.5V	16.2V
Control/ charging	17V	12V	16.2V	12V
Inverter	12V	1kVA	12V	1kVA

A critical look at table 2 shows that the values obtained at both design and simulation stages shared extreme parallelism. The deviation between design and simulation outputs of the voltage multiplier was 4.7%, within acceptable limits for electronic simulation of hybrid energy harvesters even though this difference was completely eliminated by the control mechanism attached to this system. The inverter output of 1kVA is consistent for both stages. It is also within the allowable global standard and shares consistency with Olusegun et al (2014) and Achilihu et al (2024). The 1kVA output achieved surpasses the 28V and 34V reported by Kyrillos et al. (2016) and Anis et al. (2019) respectively. Demonstrating improved performance of the designed system under controlled simulation conditions

Discharge duration of the designed system

$$\text{Duration} = \frac{\text{Battery power rating}}{\text{Total load}} \quad (8)$$

Power rating of the battery used = 12volts, 60ampere per hour

Table 3: Discharge Duration of the Designed System

Load	**Total Power (Watt)**	**Time (Hours)**
Six 40Watts bulb	240	3
Laptop + Six 40Watts bulb	300	2.4
Laptop + Six 40Watts bulb + 3 Handset charger	360	2

Table 3 shows the validity and reliability test results of the system in terms of the time duration when the various loads are attached appropriately. The time given, is the maximum time the system will work with corresponding loads before the system's battery drops down to below 5v. At this point, the battery needs to be charged. But if there is a continues flow of Noise (>85db) in the environment, the system will give continuous electricity at the output while charging the battery. This shows that the system is working perfectly under ideal environment.

CONCLUSION

This study establishes that piezoelectric transducer-based harvesters can effectively convert ambient acoustic energy into usable electrical power, presenting a viable solution for low-power, off-grid applications. Simulation results under controlled acoustic input (~85dB) indicate notable conversion potential, though real-world fluctuations necessitate adaptive circuitry and efficient energy management. Estimated performance, benchmarked against conventional harvesters (2–10% efficiency), suggests scope for optimization through improved transducer density, material stability and environmental resilience. Future work should integrate durability modeling and adaptive control to advance the use of piezoelectric systems in sustainable energy infrastructures.

REFERENCES

Achilihu, D., Oluwafunso, O. O., Akinwumi, J., and Onwunta (2024): Design and fabrication of a 1kVA power inverter. *IEEE 5th* International Conference on Electro-Computing Technologies for Humanity. *https://doi.org/10.1109/NIGERCON62786.2024.10927403*

Akorede, M. F., Ibrahim O., Amuda S. A., Otuoze A. O., and Olufeagba, B. J. (2017): Current status and outlook of renewable energy development in Nigeria. *Nigerian Journal of Technology (NIJOTECH)*, 36(1):196 – 212. http://dx.doi.org/10.4314/njt.v36i1.25

Anis, M. M. A., Farahiyah, M., Maizul, I., and Aznizam, A. (2019): Power generation by using piezoelectric transducer with bending mechanism support. *International Journal of*

Power Electronics and Drive Systems, 10(01):562 - 567. http://doi.org/10.11591/ijpeds.v10.i1.pp562-567

Dhananjay, K., Pradyumn, C., and Nupur, J. (2014): Piezoelectric Energy Harvester Design and Power Conditioning. *IEEE Students' Conference on Electrical, Electronics and Computer Science*, Pg. 2-7. https://www.researchgate.net/publication/264048646

Kadandani, N. B., Hassan, S., and Abubakar, I. (2023). Solid-state transformer (SST) and the challenges of the future grid. *FUDMA Journal of Sciences*, 7(3), 330–335. https://doi.org/10.33003/fjs-2023-0703-1965

Kenneth, E. O. and Ibe, A. O. (2010): Assessment of Electrical Energy Demand in Nigeria. https://www.researchgate.net/publication/277020538

Koteras, D. and Tomczuk, B. (2024). Three-dimensional numerical field analysis in transformers to identify losses in tape-wound cores. *Sensors (Basel)*, 24(10), 3228. https://doi.org/10.3390/s24103228

Kyrillos, K. S., Ayman, H., Yehia, H. M., Fathy Z.A. and Ahmed, M. E. (2016): Acoustic Energy Conversion into Useful Electric Energy from Disk Jockey by Using Piezoelectric Transducers. *Conference Paper*. *https://doi:10.1109/MEPCON.2016.7836998*.

Niraj, P., Anuj, G., Ebin, B. and Santhosh, N. (2014): Footstep Energy Harvester Using Piezoelectric Transducer. *International Journal of Latest Research in Science and Technology*, 3(12): 54-56 https://www.researchgate.net/publication/329557732.

Najimaldin, E. H. (2024): Noise Pollution and its effects on human health: A review. *International Journal of multidisciplinary Research*, 10(11):24. https://dio.org/10.36713/epra18872

Nkwocha, M.C., Adejumobi, I. A. and Adebisi (2024): Assessment of residential electrical energy demand for effective load management and energy conservation: Ikeja electricity distribution company network as a case study. *American Journal of engineering research,*13(05):129 - 133 *www.ajer.org*

Oluwatoyin A. S. (2023): Energy Crisis and renewable potentials in Nigeria: A review. *Science Direct*, 188(113794). https://dio.org/10.1016/j.ser.2023.113794

Olusegun, O. O, Segun, O. O. and Taiwo, R. O. (2014): Design and construction of 1KW (1000VA) power inverter. *Innovative Systems Design and Engineering*, 5(2):1-13. https://www.researchgate.net/publication/305618160

Onuu, M. U. (2020): Acoustic energy harvesting in Nigeria: prospects, technical problems and socio-economic obstacles. *Journal of Energy Research and Reviews*, 5(1): 16-33. https://doi.org/10.9734/jenrr/2020/v5i130139

Pantawane, R. N., Kanchan, V. M. and Namrata, S. K. (2017): Effects of noise pollution on human health. *International Advanced Research Journal in Science, Engineering and Technology*, 4(3):1-3

Poornanand, K., Aaditya T., Daksha B. and Neetha, K. (2017): Analysis of conversion of noise to electrical energy in a stadium. *International Journal of Industrial Electronics and Electrical Engineering*, 5(9):39-42. http://iraj.in

Predescu, D. M. and Ronu, N. G. (2025). Solid-state transformers: A Review—Part II: Modularity and Applications. *Technologies*, 13(2):50. https://doi.org/10.3390/technologies13020050

Revathi, G. and Ingitham, R. (2012): Piezoelectric energy harvesting system in mobiles with keypad and sound vibrations. *International Journal of Engineering Research & Technology (IJERT)*, (1):1-4. www.ijert.org

Satvik, S., Yash S., Bhavika P., Manimala, and Sherry, V.(2020): Converting Sound Energy to Electricity. *International Journal of Technical Research & Science (Special Issue)*, pg. 23-30. https://doi.org/10.30780/specialissue-ICACCG2020/037

Suhas, D., Sharanabasappa, C.S. and Hanumesha, P. (2019): System to transform sound energy into electricity. International Conference on Nanotechnology and Nanomaterials for Energy and Environment. *SSRN. Electronic Journal*, Pg.1-8. https://ssrn.com/abstract=3492946

Wang, W., Tang, L. and Yang, Y. (2017): Nonlinear piezoelectric energy harvesting from ambient acoustic excitations. *Applied Physics Letters*, 110(16), 163901. https://doi.org/10.1063/1.4980117

Zaharaddden, M. and Aliyu, B. (2025). Design and construction of 500 W solar generator kit. *FUDMA Journal of Sciences*, 9(6):314–321. https://doi.org/10.33003/fjs-2025-0906-3644.